Challenge Journal of Concrete Research Letters

Case Study

Cause of distress of an old building through analytical and micro–analytical methods – a case study

Rajappan Preetha [a,*], Kalpana Kumari [a], Balakrishnan Sakthi [a], Chandrasekharan Nair Harikumar [a], Haneef Ibrahim Abdul Gani [a]

[a] *Indira Gandhi Centre for Atomic Research, 603102 Kalpakkam, Tamilnadu, India*

ABSTRACT

The case study pertains to the methods such as nondestructive, semi-destructive, chemical, electrochemical and micro-analytical, utilized to assess the cause of cracking and spallation of a reinforced concrete building near to the eastern coastline of India. Cause of degradation of the structure is assessed to arrive at the appropriate repair methodology. From the analysis methods, direct cause of failure could not be attributed to a single cause since many factors co-exist such as structural cracking, carbonation and presence of chloride and the synergistic effect; hence concludes that an appropriate repair methodology has to be evolved to address each issue.

ARTICLE INFO

Article history:
Received 7 September 2022
Revised 27 October 2022
Accepted 4 November 2022

Keywords:
Concrete
Corrosion
Reinforcement
Chloride
Carbonation

1. Introduction

Technical service life of a reinforced concrete building is the time in service at the end of which structural safety is unacceptable due to either material degradation or exceedance of the load carrying capacity or both, in which case repair strategy may be adopted if it is still economically more advantageous than replacement, as mentioned in ACI 365.1R (2000). Cause of degradation of the structure is to be assessed to arrive at the appropriate repair methodology. The process of chemical and physical deterioration of concrete with time is a function of presence and transport of deleterious materials in concrete and the synergistic effect of applied loads as well explained in his review by Ahmad (2003). The rate and extent of this transport is largely dependent on concrete pore structure, presence of cracks and the microclimate of the surface of concrete. Though the coefficient of permeability of concrete is dependent on concrete materials and the method of execution, it is also influenced by age. Major reason as mentioned in Dhawan et al. (2014) for deterioration of a reinforced concrete building is the reinforcement corrosion which is usually manifested as cracking, staining and spallation. This highlights the importance of in service inspection and routine maintenance of buildings.

The case study pertains to an office building built in the 1970s.This building is within 1km of the eastern coast line of India. This is a highly corrosive belt of peninsular India as per Natesan et al. (2005). The building serves as the main design office and has always been the most utilized office space in a power plant campus. Being one of the first buildings in the campus, several novel architectural features like slender columns, waffle slab, hanging staircase and long wide windows with deep sunshades were conceived to give a perfect ambience of a well ventilated design office with natural light. The basis of analysis and design of the structure is the national standard, IS 456 (1968) of the early '70s. The structure has seen a life span of 48 years with proper maintenance. It has been observed recently that, few of the reinforced concrete columns have started cracking and spalling just above the ground level. The distress in columns started with vertical cracking in the cover region, followed by spallation. This study aims at estimating the extent and type of degradation of the building analytically and micro-analytically (Qazweeni et al.) and interpreting the results.

* *Corresponding author*. Tel.: +91-944-412-9806 ; Fax: +91-044-274-80306 ; E-mail address: predinesh@igcar.gov.in (R. Preetha)
ISSN: 2548-0928 / DOI: https://doi.org/10.20528/cjcrl.2023.01.003

2. Structural Layout of the Building

The building is a reinforced concrete (RC) framed construction with brick masonry infill. It is an H –shaped double-storied structure with parallel plan dimension of 72×13.6 m and a connecting corridor. The height of each floor is 3.575 m. Each arm of the building is structurally separated using expansion joints. Fig. 1 shows the schematic representation of the section and plan of building. At plinth level viz. 0.6 m from ground level, longitudinal beams are provided and there are no transverse plinth beams. Foundation is at 1.5 m from ground level. Geometrical details of beams, columns and slabs are provided in Table 1. The longitudinal beams are provided above the windows and not at the floor level, whereas transverse floor beams are provided at floor level. From the sectional drawings, it is learnt that the load bearing masonry and the RC columns (Fig. 1a) were provided to share the floor loads. The grade of concrete used was M20 and grade of steel Fe 415.

Table 1. Sectional properties of beams, columns, and slab.

Member	Size
Longitudinal floor beams	230×600 mm
Transverse floor beams	150×410 mm
External column	150×500 mm
Internal column (plus geometry)	150×300 mm
Longitudinal plinth beams	230×300 mm
Transverse plinth beams	230×450 mm (only at two ends)
Slab	65 mm thick

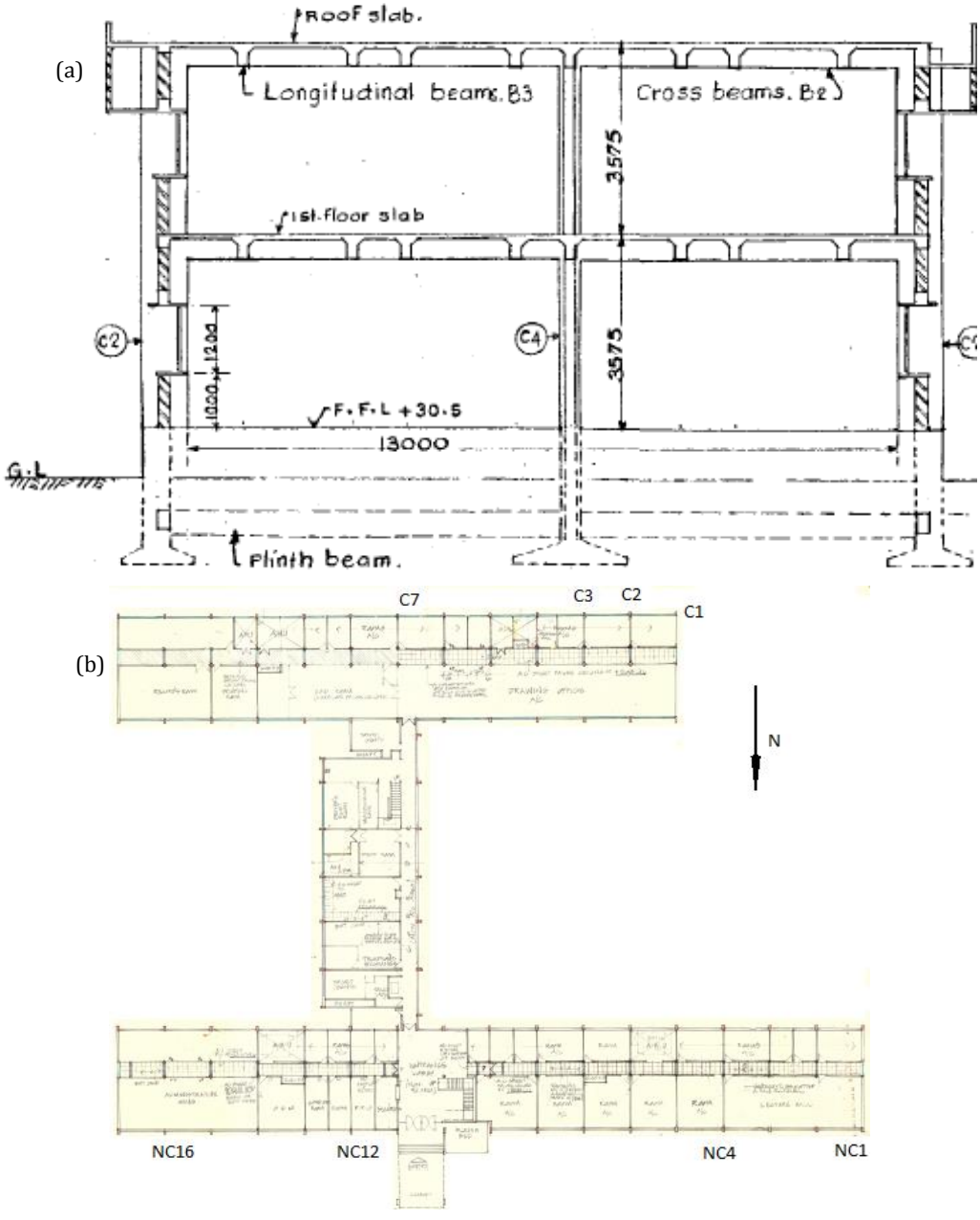

Fig. 1. (continued)

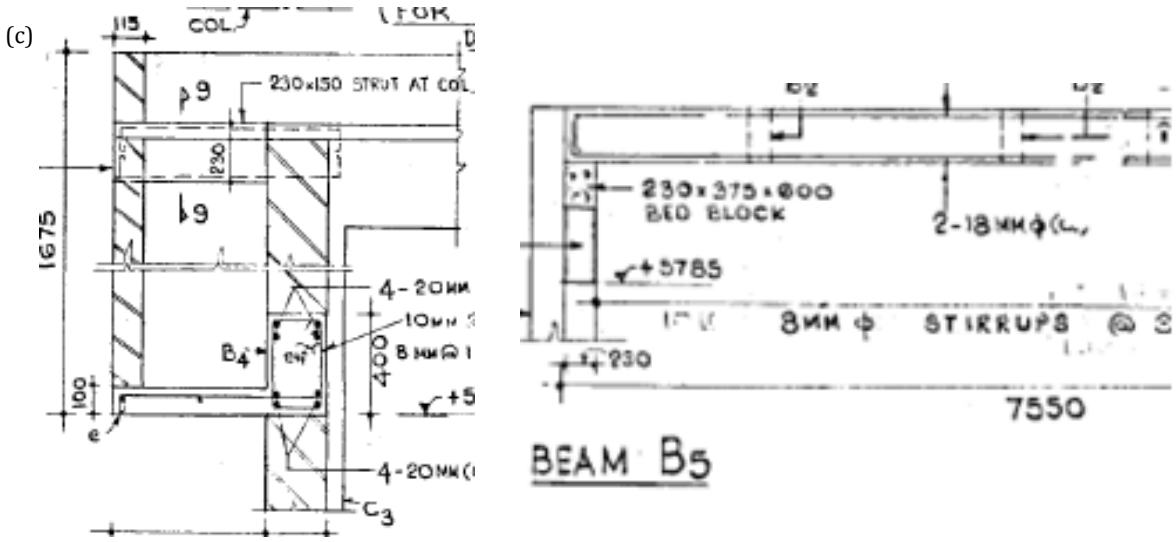

Fig. 1. a) Sectional details; b) Plan of the building; c) Cross-section of floor beams and load-bearing masonry.

3. Assessment Methodologies

3.1. Visual inspection

Visual inspection generally is the primary method used as a first step in assessing the condition of the structure. An expert visual inspection of exposed concrete and masonry helps to detect and define areas of ageing-related distress that result in visible effects on the surface. To begin with, a team of experts inspected both the ground and the first floor of the building. The team evaluated the beams and slabs for explicit visual cracks and other distress in the structural members. During the visual inspection, the nondestructive tests required for precise evaluation of the structures, were also determined.

Fig. 2. Spallation of columns: a) C1; b) C2; c) C3; d) C4.

Fig. 3. Cracks in masonry and sunshades.

The cracks which lead to spallation were more than 2-3 mmand length of 400 mm, whereas hairline cracks of the order of 0.5 mm were also visible. However, initially, cracking and spallation appeared to be due to corrosion, aspect of overloading or settlement of the founding medium etc. could not be overruled. The soil reports from recent adjacent construction site were useful in overruling the issue of settlement of the footing. It was further decided to analyze the frame of the building for the current loading and investigate the condition through non-destructive, semi destructive, electrochemical tests, chemical analyses and X-Ray Diffraction (XRD) etc. as shown in the Table 2. The flow chart depicts the various stages undertaken in the present survey (Fig. 4).

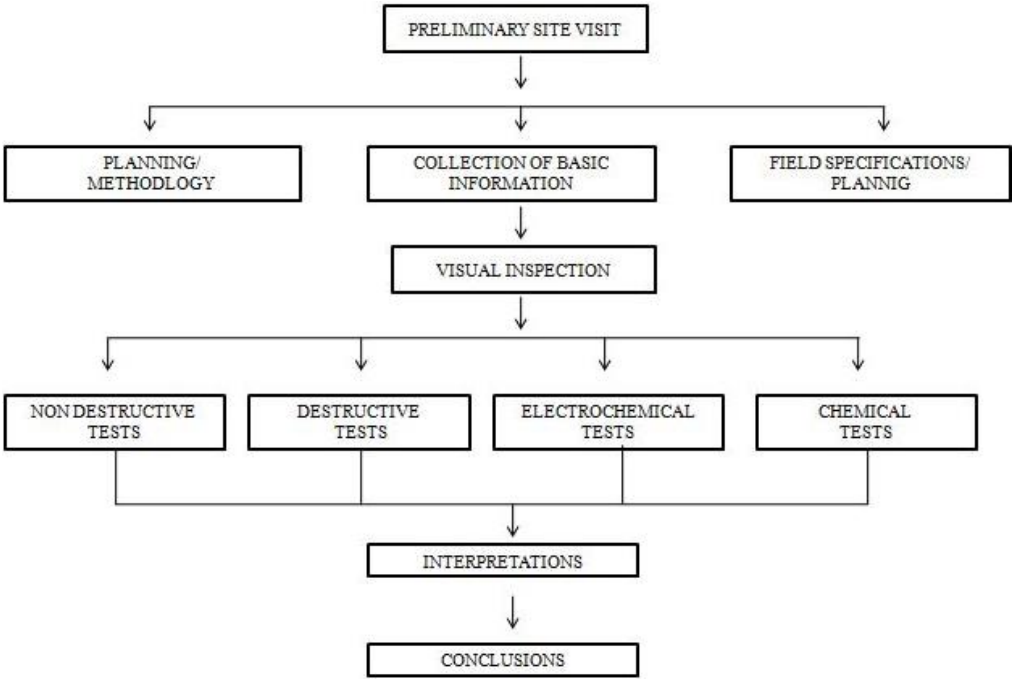

Fig. 4. Flow chart of survey.

Table 2. Condition assessment methods.

Material and characteristic	Column A (*t*)
Concrete / masonry	
General quality	Ultrasonic pulse velocity
Cracking / spalling	Visual inspection, ultrasonic pulse velocity
Strength	Rebound hammer test, ultrasonic pulse velocity
Microbiological assays	Microbially induced corrosion
Concrete reinforcement	
Location of reinforcement	Rebar locator
Corrosion	Visual inspection, electrical resistivity
Concrete durability	pH of the concrete, chloride content detection by titration, carbonation test, RCPT
Micro-chemical analysis	XRD of the concrete samples
Groundwater / soil quality	Chemical analysis, XRF analysis

3.2. Structural analyses

Building is evaluated by modelling and analysis to check the structural capacity of the structure against gravity loading conditions such as dead and live loads. The structural analysis is done using an engineering software .The structure is idealized as a 3D frame, using 3D beam element for columns and beams. Fig. 5 represents the model of the building for the analysis. The member capacity have been calculated using limit state methods given in national code IS 456 (2000), SP-24 (1983) and also ACI 318 (2008). As the structural analysis is to assess the cause of distress, only the dead load and live load as per code IS 875 (1987), and their combination with a partial safety factor of unity is considered.

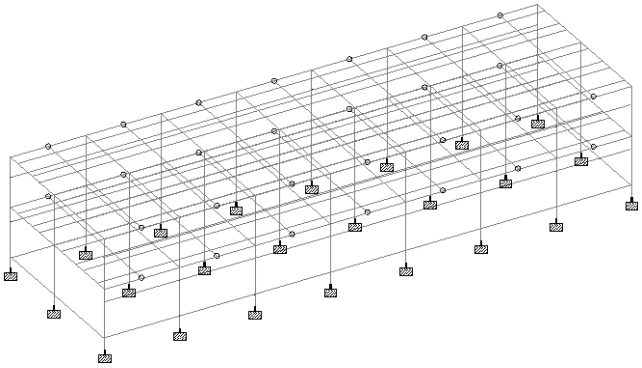

Fig. 5. Partial model of the building.

3.3. Field tests

Locations for performing NDT examinations of rebound hammer, ultrasonic pulse velocity and resistivity were identified on the basis of the environmental exposure conditions viz. coastal environment and distress observed etc. In the overall assessment area totally 26 sampled test points such as external/internal columns and masonry were selected such that the points encompass both the potentially affected areas as well as areas from unaffected portion of the structure, so as to serve as baseline or control.

3.3.1. Rebound hammer test

Schmidt rebound hammer is a simple, handy tool, which can be used to provide a convenient and rapid indication of the compressive strength of concrete. When the plunger of rebound hammer is pressed against the surface of concrete, a spring controlled mass with a constant energy is made to hit concrete surface to rebound back. The extent of rebound, which is a measure of surface hardness, is measured on a graduated scale. This measured value is designated as Rebound Number (rebound index). This is further converted to compressive strength of the material subjected to test. The rebound hammer testing was carried out as per IS 13311 (Part 2) (1992) using Proceq make DIGI-SCHMIDT 2000 concrete test hammer of Model ND/LD. Around each point of observation, nine readings of rebound indices were taken and the average compressive strength was displayed for the point of observation.

3.3.2. Ultrasonic pulse velocity (UPV) test

UPV test is used to measure the velocity of ultrasonic waves inside the concrete to establish the homogeneity and integrity of the concrete, the presence of cracks, voids and other imperfections and the quality of concrete in relation to standard requirement. Ultrasonic instrument used for testing was Proceq Tico ultrasonic instrument which is handy, battery operated and portable instrument. The electronic pulses are generated by the transmitting transducer and collected at the receiving transducer, and the travel time between the two transducers is measured electronically. Grids were made on the selected location, just opposite/adjacent as required to the selected location. The transducer was put on the selected grid on the location and the receiving transducer on the opposite/adjacent grid location after greasing the surface to prevent any air gaps between the testing surface and the transducers. General criterion for concrete quality grading is given in Table 3.

Table 3. Criterion for concrete quality grading as per IS 13311 (Part 1) (1992).

S.No.	Velocity criterion by cross probing (km/sec.)	Concrete quality grading
1	above 4.5	excellent
2	3.5 to 4.5	good
3	3.0 to 3.5	medium
4	below 3.0	doubtful

3.3.3. Resistivity testing of concrete

The electrical resistivity is defined as the ratio between the applied potential and the current circulating between two electrodes providing the arrangement which enables the calculation of the geometrical characteristics. The electrical resistivity is an indirect measurement of the porosity and the connectivity of the pores. It is used to detect wet areas in the concrete and therefore is used to assess the probability or likelihood of corrosion of the reinforcement bar. One of the commercial equipment available for measurement of resistivity of concrete is, Resistivity Meter, which is a four probe device. This is based on the classical four electrode system in which four equally spaced electrodes are electrically connected to the concrete surface. Proceq make Resipod which is a fully integrated 4-point Wenner probe based on Rilem TC 154-E (2000) was used for testing.

Table 4. Interpretation of resistivity results as per RILEM TC 154 (2000).

Resistivity (ρ) range in kΩcm	Risk of corrosion interpretation
< 10	high
10 to 50	moderate
50 to 100	low
> 100	negligible

3.4. Laboratory tests – chemical analysis

At the sites of distress, the spalled concrete was removed and tested for carbonation, pH and chloride penetration. The 6 mm stirrups were fully corroded, while there was a reduction in diameter at the main bar of 22 mm diameter. At one of the columns, the spalled concrete was showing biogenic growth at the inner surface. Hence the sample was tested using microbiological characterization. The topsoil which was covering the columns at the location of distress was also analyzed in the lab using chemical analysis and X-ray Fluorescence. One

of the columns was exposed up to foundation to check the condition below the ground. There was no distress found in the embedded columns and foundation. Water and soil samples were collected from the foundation and tested for sulphates, chlorides or any other harmful chemicals. Spalled, drilled concrete and cored samples were tested for chloride content and pH; further cover concrete was removed for assessing the status for rebars. Rapid chloride penetration test was attempted to determine the permeability of concrete.

3.4.1. Test for chloride content of concrete

The presence of chloride in the concrete is the contributory factor towards corrosion of reinforcement. The chloride content of concrete can be determined by chemical analysis of concrete in the laboratory. The significance of this test is to understand the chloride content present in the concrete and also chloride profiling with depth, to establish whether the source of chloride contamination is internal or external. The chloride content in concrete was determined from broken core samples of the concrete member, in accordance with IS 14959 (Part 2) (2001). As per IS 456, the maximum total Acid Soluble Chloride content for reinforced concrete or plain concrete containing embedded metal is 0.6 kg/m^3. pH was determined using Hanna make HI991300 model portable pH meter.

A colorimetric method based on Collepardi (1995), by spraying Fluoresceine and a Silver Nitrate solution was used to determine the presence of free and bound chloride and its penetration into the concrete structure as it has been generally assumed that free chloride ions can promote the corrosion process of steel reinforcement. In brief, the investigation was carried out at the fractured surfaces of the structure by spraying the Fluoresceine solution (1g/L in a 70% solution of ethyl alcohol in water) followed by Silver Nitrate (0.1mol/l) aqueous solution. A dark pink coloration indicated presence of free chloride areas and a dark brown coloration indicated bound chloride zone on the grey concrete (Fig. 6). This process was also adopted on a fractured core sample extracted from the structure, wherein the depth of free chloride penetration was indicated by a color change with a clear demarcation till the region of bound chloride region.

Fig. 6. Colorimetric method to check free and bound chloride on the exposed structural member.

3.4.2. Rapid chloride penetration test(RCPT)

A cylindrical core specimen (200×100 mm) was typically cut as a slice (50×100 mm) and used for this test. The RCPT apparatus consists of two reservoirs. The specimen was fixed between two reservoirs using an epoxy bonding agent to make the test setup leak proof. One reservoir (connected to the positive terminal of the Direct current (DC) source) was filled with 0.3N NaOH solution and the other reservoir (connected to the negative terminal of the DC source) with 3% NaCl solution. The terminals were then connected to the 60 V DC power supply and the current reading in mA was recorded for every half an hour up to 6 hrs. The total charge passed during this period was calculated in terms of coulombs using the trapezoidal rule as given in the ASTM C1202 (2019).

3.4.3. Carbonation

The carbonation test was carried out as per RILEM CPC-18 (1988). The reduction of the pH value could be made visible by applying a 1% phenolphthalein solution to a freshly fractured surface of concrete. The non-carbonated areas turn red or purple while carbonated areas remain colorless. The phenolphthalein solution was sprayed on the freshly cored concrete surface and the color change was observed (Fig. 7).

3.4.4. Microbiological assays

The spalled concrete from C3 column had a pale yellow color deposition (Fig. 8). The deposit was sliced and observed under a light microscope for microscopic structures. Fungal cells in spalled concrete and soil re-

sembled of Gaeumannomycella / Gaeumannomyces sp. and hyphopodia and also sulphur reducing bacteria. This was confirmed by using the deposit as an inoculum for microbial enrichment in Saboraud dextrose broth and Luria-Bertani broth. Sulphur was not present in X-Ray fluorescence (XRF) analysis of the deposited sample.

Fig. 7. Concrete carbonation tests on the fractured structural member, cored member and checking for the corrosion of rebar.

Fig. 8. Biogenic growth at the inner face of the column.

3.4.5. X-ray diffraction (XRD) of concrete samples

XRD data were acquired on Intel make machine (Model - Equinox 2000) equipped with Gas Detection Cell (Argon and Ethan) detector and intensity measurements were carried out using germanium mono-chromated Cu-Kα radiation (λ=1.789 A^0) in asymmetric acquisition mode. XRD involves directing an incident wave into a material and recording outgoing diffracted wave direction and intensity using a detector. Scattered waves emitted from an atom of different type and position, interface constructively or destructively along different paths. The crystal structure of a material is related to this diffraction pattern. By scanning, a sample in 2θ range, all possible diffraction directions is obtained. The crystal phases of crushed concrete specimen were determined by correlating the change in intensity in the field of 10-80° of 2θ. Crystalline phases identified from the standard database, JCPDS (1985) and literature.

4. Results and Discussion

4.1. Visual inspection

Though cracking was not visible at first, except for in few columns in the southern block, close inspection revealed hairline cracks and also signs of repairs previously carried out in several columns. Except for the south block, plinth protection and drain covered the columns all around the periphery. The south block columns showed distress to a height of 0.8 m from the ground level. Organic soil was observed to cover this particular height of the column for quite some duration and distress became visible on removing the soil cover. Roughcast plastered external masonry, though appeared intact outside; cracking was seen at the inner surface. There was visible distress in masonry and window panes associated with the columns. There were no evident signs of distress in the internal beams and columns.

4.2. Structural analyses

The external columns were found to be sway columns with a slenderness ratio exceeds 22 in both directions, according to ACI 318 (2008). Axial loads in the columns were exceeding the Euler critical load applying the stiffness variation in columns due to cracking, creep and column non-linearity (Figs. 9-11). Hence peripheral columns (150×500 mm) were failing due to instability and buckling.

4.3. Nondestructive tests

Rebound hammer and UPV were resorted to identify the condition of masonry, initially, at areas where there were no visible defects (Table 5). With these readings as reference, the tests were conducted at areas where hairline cracks were visible in masonry. The range of UPV at good locations was 3450-4450 m/s using the direct transmission method and 2880-3220 m/s using the surface transmission method. At regions where cracking was seen, the UPV dipped to 2600 m/s which show degradation. The compressive strength obtained from rebound hammer, both for concrete columns /beams and masonry were in the range 35-45 N/mm^2.

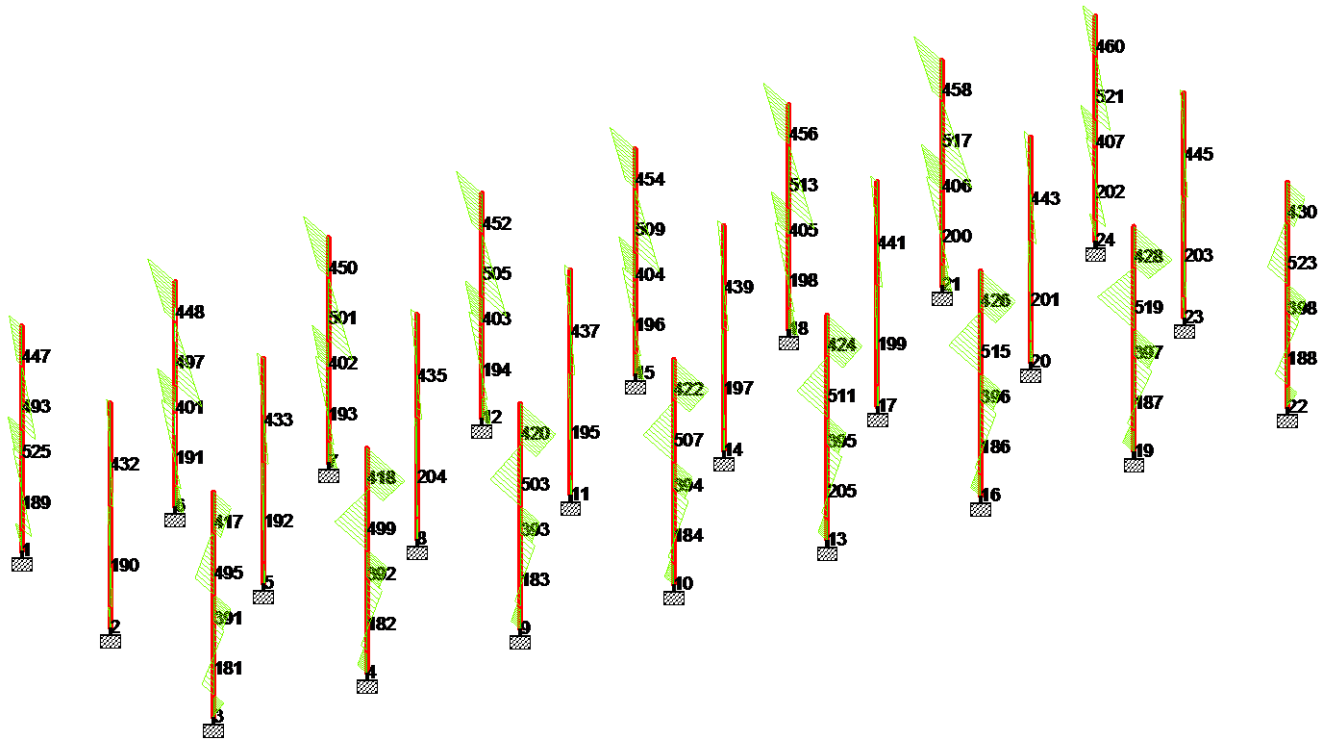

Fig. 9. Column bending moment along the major axis due to static loads.

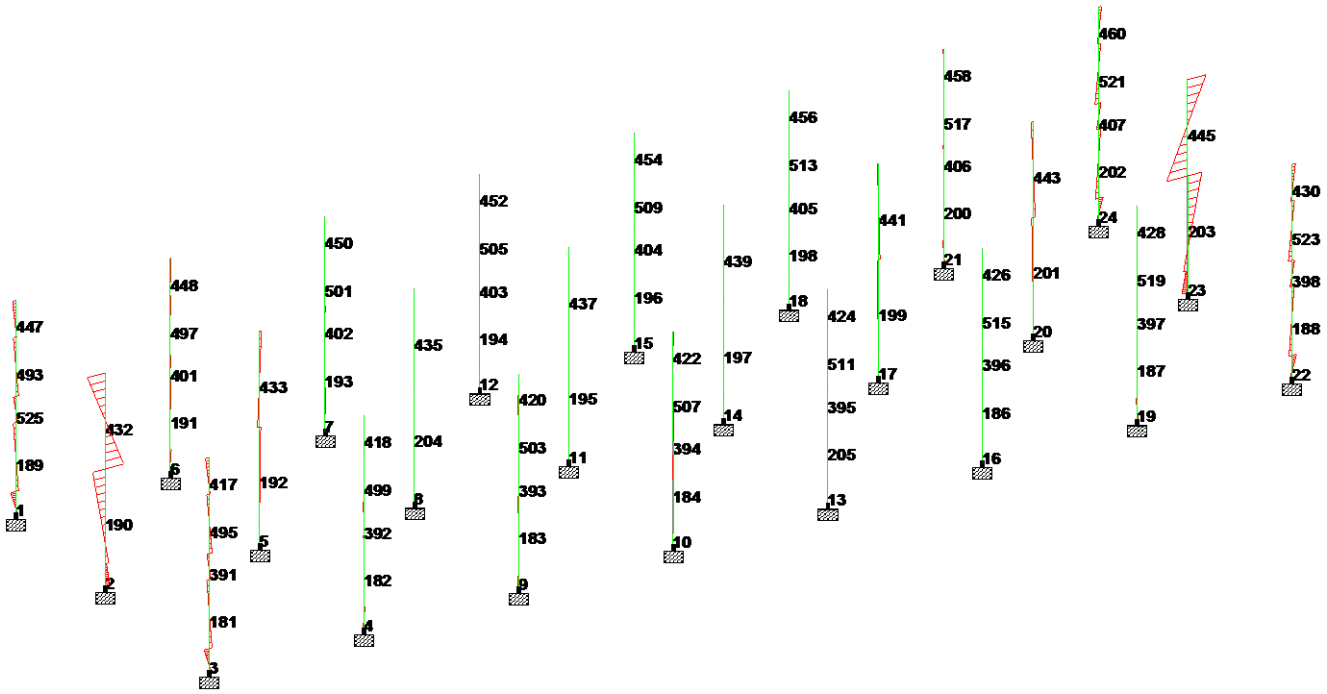

Fig. 10. Column bending moment along the minor axis due to static loads.

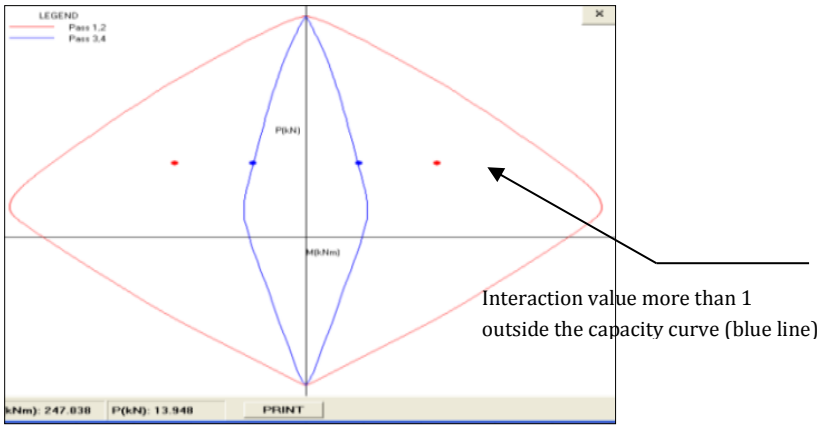

Fig. 11. Interaction chart by using the additional moment method as per ACI 318 (2008).

The external columns were further tested after validating the healthiness of columns inside the building. The columns showed reduced UPV values in the range of 2320 m/s near the distress, 4700 m/s at -0.9 m from ground level, 4660 & 4460 m/s at -0.6 m and -0.3 m levels respectively. Just above the distressed area also the UPV was as high as 4240 m/s. These values prove that the distress is highly localized. The distressed area was dry hence half-cell potential measurements when tried gave only positive potentials. Even resistivity measured in the distressed columns showed high values. But below ground, the resistivity dipped to 33-67 K ohm-cm, which is due to moisture in the soil. UPV conducted on external columns at the north block rendered values of 4000-3500 m/s, suddenly dipping to 3300 m/s at the hairline cracks.

Table 5. Results of the nondestructive tests.

S.No.	Location	Rebound hammer values (N/mm^2)	UPV (m/sec)
1	C2 column +0.6 m from crack	40.0	3820
2	C3 column +0.3 m from crack	40.0	4240
3	C3 column near crack	38.8	0-2320
4	C3 column-0.9m from crack	44.3	4700
5	C3 column- 0.6m from crack	39.0	4660
6	C3 column -0.3m from crack	43.3	4460

Table 6. Chloride and sulphate in founding medium.

Ion	Concentration (%)
Chloride	0.0055
Sulfate	0.0066

Table 7. Elemental composition in founding medium-XRF.

S.No	Element	Concentration (%)
1	Al	3.91 ±0.01
2	Si	24.17 ±0.12
3	Ca	3.06 ±0.18
4	Fe	3.26 ±0.12

4.4. Chemical analysis

Tables 6 and 7 gives chloride, sulphate and elements in soil. Table 8 gives analysis results for carbonation, chloride penetration and pH of spalled concrete samples. Chemical analysis showed high chloride content on an average 1.4 kg/m^3 in external concrete columns and 0.9 kg/m^3 at internal columns, which was almost uniform with depth. Carbonation levels at ground level of external columns were very high whereas carbonation at inner columns and beams and upper elevations of external columns was nil. The total charge passed through the concrete specimen in RCPT was 5000 Coulombs which shows high chloride ion penetrability of concrete.

Chloride ions can get introduced into concrete through raw materials such as aggregate, mixing water (internal chloride) and admixtures or from chloride sources in the service environment (intruded chloride). Calcium chloride was prevalent as an accelerating admixture in concrete in 1970s as given in Clarke (2009) to increase the rate of early strength development, reduce the setting time or to increase the production rate in precast industry according to Chen (2017). When concrete is contaminated as a result of the use of calcium chloride, it is identifiable by an even distribution of the chloride content between 0.5 and 1% by mass of cement as per Brueckner et al. (2017) and Kim et al. (2018) (as recommended $CaCl_2$ was less than 1.5%). When concrete is contaminated due to external sources the chloride profile decreases from the face of exposure to interior. Gebregziabhier (2008) explains that the internal chloride ions affect the hydration process and hydration products of cementitious materials as they get introduced in fresh state, while the external chloride alters the pore structure and solid/ liquid phase composition within concrete. Once inside concrete, chloride assumes any three states, free chloride in bulk pore solution, physically adsorbed chloride on the surface of hydration products or chemically bound chloride by solid phase. The chemically bound chloride results in decrease of porosity by formation of Friedel's salt ($3CaO\_Al_2O_3\_CaCl_2\_10H_2O$) and Kuzel's salt ($3CaO\_Al_2O_3\_0.5CaCl_2\_0.5CaSO_4\_10H_2O$). With carbonation, there is decrease in concrete alkalinity from pH 12.5–13 towards pH 9 and during this process bound chlorides are released back into solution, which increases the free chloride content over time (Eq. (1)). Ettringite also does not exist in severely carbonated concrete as its stability is also pH dependent.

$$3CaO.Al_2O_3.CaCl_2.10H_2O + 3CO_2 \rightarrow 3CaCO_3 + 2Al(OH)_3 + CaCl_2 + 7H_2O \quad (1)$$

So in carbonated environment the carbonation progresses to the depth of the reinforcement and the protective layer on the steel destabilizes causing initiation of corrosion in the presence of oxygen and moisture or the release of chlorides into the pore solution may exceed the critical chloride threshold and cause corrosion before the carbonation front reaches the reinforcement. Corrosion of reinforcement causes the formation of voluminous reaction products which can cause spalling and delamination of the concrete cover. According to Kim et al, in cement the content of C_3A and C_4AF dominates the chemical binding of chloride ions, while C_3S and C_2S dominates physical binding. Hence threshold chloride content can vary with type of cement, depending on the C_3A and C_4AF content. The reaction of C_3A with chloride forms Friedel's salt, which removes free chlorides from the pore solution and thus not participate in the corrosion process. Thus high concentration of C_3A is inhibits chloride-induced corrosion of steel in concrete. And it is also seen that internal chloride showed higher chloride threshold than external chloride, as lesser amount of free chloride participate in the corrosion process, due to chloride binding in the initial hydration stage.

4.5. X-ray diffraction of the concrete samples

XRD of fresh concrete usually shows (Fig. 12) the crystalline peaks of hydration products, Calcium hydroxide, gypsum, ettringite, continuous bumps of calcium silicate hydrate gels, calcium carbonate etc. and quartz phase from aggregate and cement. In the sample, calcium hydroxide or Portlandite phase at 2θ angle of 18 & 34° were missing, which were replaced by peaks at 2θ angle of 23-25°,26-27°,39-40°, 78°, as calcite/vaterite and aragonite according to Stutzman (2010), the polymorphs of calcium carbonate. Calcite which is in abundance in the 40 mm layer of the concrete is the most stable polymorph. Vaterite is in concrete due to the high ambient temperature at site and aragonite, due to the presence of chloride as given in Ramakrishna et al. (2016). Other crystalline products identified were bassanite ($CaSO_4.5\,H_2O$) (at 2θ angle of 20.72°, 23.23°, 29.7°, 42.45°), and langbeinite (potassium magnesium sulphate etc.) (at 2θ angle of 21.92°, 25.39°, 26.93°, 31.2°, 39.55°, 41.69°, 43.1°).These are products formed due to the instability of gypsum and ettringite in carbonated environment along with high temperatures. Quartz phase from 2θ angle of 20.85°, 26.65°, 36.54°, 39.46°, 50.14°, 60° and 68° were evident in some samples of external/internal columns, but not in all which shows some ageing. Calcium monosulphates (2θ angle of 10.2°) and Friedel salt (2θ angle of 11.05°) also appeared in some inner layers of samples as given in Hashimoto et al. (2012), Fujiwara et al. (1992), Florea et al. (2012), and

Suryavanshi et al. (1996). The peaks at 2θ angle of 13-14° indicate free chloride. Ettringite peaks at 2θ angle of 23.5° were seen in the sample of C3 column, having biogenic growth.

Table 8. Chloride content and pH of concrete.

S.No.	Sample no.	Average chloride	Average pH	Estimated depth of carbonation
1	C2 + 0.8 lvl	1.239	8.955	40-50 mm
2	C3 + 0.8 lvl	1.415	10.805	40-50 mm
3	C7 + 0.8 lvl	1.365	10.115	
4	C2 + 4.75 m	0.885	10.40	
5	C3 + 4.75 m	1.504	11.58	
6	C7 + 4.75 m	1.482	10.87	
7	NC1 + 0.8 lvl	1.4891	10.29	20 mm
8	NC4 + 0.8 lvl	1.5147	11.46	20 mm
9	NC12 + 0.8 lvl	1.5051	11.60	15 mm
10	NC16 0lvl	0.4378	10.79	40 mm
11	NC4 + 1.75 m	0.806		0
12	NC4 + 4.75 m	0.993		0
13	NC16 + 4.75 m	0.250		0
14	NC16 + 1.75 m	1.613		2 mm
15	NC12 + 1.75 m	2.995		0 mm
16	Internal beam 1	0.791	11.52	0 mm
17	Internal beam 2	0.594	11.28	0 mm

5. Conclusions

- While checking the capacity of the structure for unfactored static load combination peripheral columns (150×500 mm) were found to be failing by instability and buckling, considering age related degradation in stiffness as per ACI 318, which leads to structural cracking of the columns. Nonlinear static pushover analysis is suggested for further structural assessment.
- Nondestructive testing validates the visual inspections that the external columns are cracking locally just above the ground. The integrity of columns just above and below this localized region was good.
- Chemical analysis showed high chloride content (1.4 kg/m^3) in external concrete columns and 0.9 kg/m^3 at internal columns. As the chloride content from surface to interior was uniform, the source of chloride is assessed to be internal, that would have admixed during hydration (say $CaCl_2$ of less than 1%). Concrete core from an inner column showed evidence of bound chloride from chemical analysis and in XRD, which explained the absence of corrosion in the internal elements, even though total chloride content was exceeding the threshold value (of 0.6 kg/m^3).
- The grade of OPC cements used in the 1970's contained high C_3A content of 10% and more as per internal quality reports and Shetty (1988), which chemically bonded chloride to Calcium chloroaluminate (Friedel salt). But XRD of spalled concrete from external columns were not showing Friedel salt peaks. The outer columns were heavily carbonated, and at high carbonation levels the Friedel salt is unstable hence breaks into free chloride which corrodes the rebars.
- The reason for higher carbonation at the lower levels of column is the structural cracking and the conjugal higher permeability based on Saeki (2002). It can be inferred that, structural instability in the columns lead to the cracks, which further increased the carbonation release of free chloride leading to corrosion of rebars, expansion, and spallation.

From the above it is inferred that, the direct cause of distress could not be attributed to a single cause since many factors co-exist such as cracking, carbonation and presence of chloride. These factors are interrelated.

Ina holistic perspective, it is concluded that, only external columns got cracked due to local effects, and internal structural elements were healthy. Considering the level of structural degradation of columns for continuing the functional requirement as per the current national standards and deterioration of material property in steel and concrete, appropriate measure for retrofit needs to be evolved, based on further structural assessment.

Acknowledgements

Authors are obliged to the labs of WSCD (BARCF), HSEG and XSCGS of Indira Gandhi Centre for Atomic Research for conducting tests for chloride, sulphates, microbiological assays, XRF and XRD which helped in the interpretation of the results.

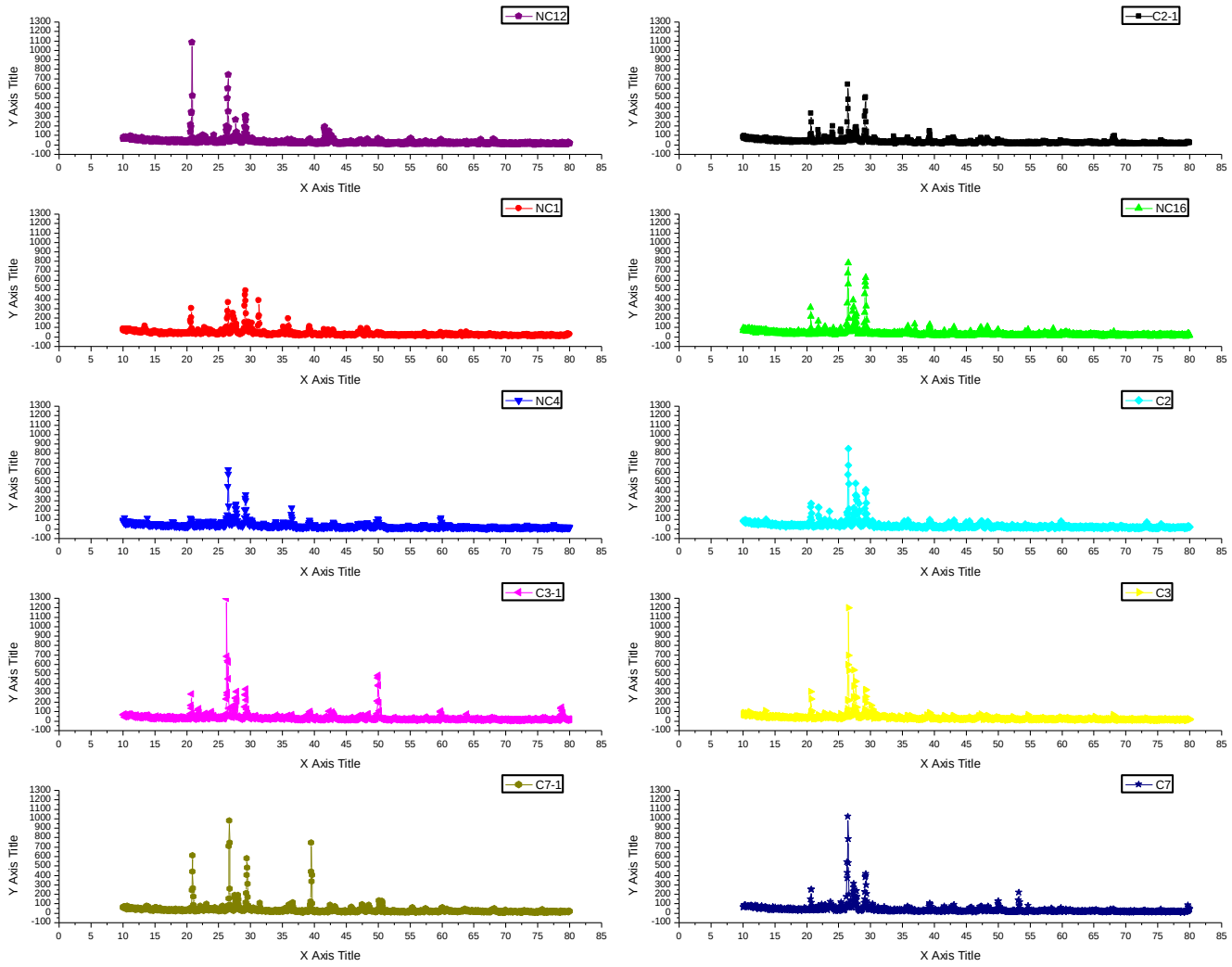

Fig. 12. XRD results the concrete samples.

Funding

The authors received no financial support for the research, authorship, and/or publication of this manuscript.

Conflict of Interest

The authors declared no potential conflicts of interest with respect to the research, authorship, and/or publication of this manuscript.

REFERENCES

ACI 318 (2008). Building Code Requirement for Structural Concrete. American Concrete Institute, Farmington Hills, Michigan, USA.

ACI 365.1R (2000). Service Life Prediction-State of Art Report. American Concrete Institute, Farmington Hills, Michigan, USA.

Ahmad S (2003). Reinforcement corrosion in concrete structures, its monitoring and service life prediction – a review. *Cement & Concrete Composites*, 25(4-5), 459–471.

ASTM C1202 (2019). Standard Test Method for Electrical Indication of Concrete's Ability to Resist Chloride Ion Penetration. American Society for Testing and Materials, West Conshohocken, PA, USA.

Brueckner R, Lambert P (2017). Unexpected effects of historic concrete innovations. *International Journal of Heritage Architecture*, 1(4), 549-563.

Chen MC, Restrepo JI (2021). Service-life performance case studies of underground reinforced concrete utility vaults. *Journal of Performance of Constructed Facilities*, 04021006.

Chilakala R, Thenepalli T, Huh JH, Ahn JW (2016). Preparation of needle-like aragonite precipitated calcium carbonate (PCC) from dolomite by carbonation method. *Journal of the Korean Ceramic Society*, 53(1), 7-12.

Clarke JL (2009). Historical approaches to the design of concrete buildings and structures. Technical Report 70, Concrete Society, Camberley, Surrey, UK.

Collepardi M (1995). Quick method to determine free and bound chlorides in concrete. *1st RILEM workshop on Chloride Penetration into Concrete*, St Rémy lès Chevreuse, France, 10-16.

Dhawan S, Bhalla S, Bhattacharjee B (2014). Reinforcement corrosion in concrete structures and service life predictions – A review. *9th International Symposium on Advanced Science and Technology in Experimental Mechanics*, New Delhi, India, 1-6.

Florea MVA, Brouwers HJH (2012). Chloride binding related to hydration products - Part I: Ordinary portland cement. *Cement and Concrete Research*, 42, 282–290.

Fujiwara Y, Maruya T, Owaki E (1992). Degradation of concrete buried in soil with saline groundwater. *Nuclear Engineering and Design*, 138,143-150.

Gebregziabhier TT (2008). Durability problems of 20th century reinforced concrete heritage structures and their restorations. *M.Sc. thesis*, Barcelona School of Civil Engineering, Barcelona, Spain.

Hashimoto K, Yokota H, Sato Y, Sugiyama T (2012). Chloride ion binding behaviour of deicing salts under freeze-thaw environment. *2nd International Conference of Microstructural Durability of Concrete Composites*, Amsterdam, Netherlands, 622-629.

IS 13311 (Part 1) (1992). Methods of Non–destructive Testing of Concrete: Part 1 Ultrasonic Pulse Velocity. Bureau of Indian Standards, New Delhi, India.

IS 13311 (Part 2) (1992). Methods of Non–destructive Testing of Concrete: Part 2 Rebound Hammer. Bureau of Indian Standards, New Delhi, India.

IS 456 (2000). Plain and Reinforced Concrete - Code of Practice. Bureau of Indian Standards, New Delhi, India.

IS 875 Part –I & II (1987). Design Loads (other than earthquake) for Buildings and Structures. Bureau of Indian standards, New Delhi, India.

IS14959 (Part 2) (2001). Determination of Water Soluble and Acid Soluble Chlorides in Mortar and Concrete – Method of Test – Part 2: Hardened Mortar and Concrete. Bureau of Indian Standards, New Delhi, India.

Kim MJ, Ann KY (2018). Corrosion Risk of Reinforced Concrete Structure Arising from Internal and External Chloride. *Advances in Materials Science and Engineering,* 2018, 1-7.

Natesan M, Venkatachari G, Palaniswamy N (2005). Corrosivity and durability map of India. Corrosion Science and Engineering Division, Central Electrochemical Research Institute, Karaikudi, lndia. https://krc.cecri.res.in

Qazweeni JA, Daoud OK (1991). Concrete deterioration in a 20-year-old structure in Kuwait. *Cement and Concrete Research*, 21, 1155-1164.

RILEM CPC-18 (1988). Measurement of Hardened Concrete Carbonation Depth. RILEM Publications SARL, 21(126), 453-455, RILEM, Marne la Vallée Cedex 2, France.

Rilem Tc 154-E (2000). Electrochemical Techniques for Measuring Metallic Corrosion. RILEM Publications SARL, 36(261), 461–471, RILEM, Marne la Vallée Cedex 2, France.

Saeki T (2002). Effect of carbonation on chloride penetration in concrete. *3rd RILEM workshop on Testing and Modelling the Chloride Ingress into Concrete*, Madrid, Spain, 381-394.

Shetty MS (1988). Concrete Technology. S.Chand & Co., India.

SP 24 (1983). Explanatory Handbook on Indian Standard Code of Practice for Plain and Reinforced Concrete (IS 456:1978). Bureau of Indian standards, New Delhi, India.

Standard X-Ray Diffraction Powder Pattern (1985). Joint Committee of Powder Diffraction Standards (JCPDS). American Chemical Society, Washington, DC, USA.

Stutzman P (2010). Direct Determination of Phases in Portland Cements by Quantitative X-Ray Powder Diffraction. Technical Note (NIST TN), National Institute of Standards and Technology, Gaithersburg, MD.

Suryavanshi AK, Scantlebury JD, Lyon SB (1996). Mechanism of Friedel's salt formation in cement rich in tri-calcium aluminate. *Cement and Concrete Research*, 26(5), 717-727.